Journal of Achievements in Materials and Manufacturing Engineering
VOLUME 37
ISSUE 2
December
2009

Processes forming the microstructure evolution of high-manganese austenitic steel in hot-working conditions

L.A. Dobrzański*, W. Borek
Division of Materials Processing Technology, Management and Computer Techniques in Materials Science, Institute of Engineering Materials and Biomaterials, Faculty of Mechanical Engineering, Silesian University of Technology, ul. Konarskiego 18a, 44-100 Gliwice, Poland
* Corresponding author: E-mail address: leszek.dobrzanski@polsl.pl

Received 20.09.2009; published in revised form 01.12.2009

Properties

ABSTRACT

Purpose: The aim of the paper is to characterise the microstructure evolution of new-developed 27Mn-4Si-2Al-Nb-Ti high-manganese steel in various conditions of hot-working.
Design/methodology/approach: Flow stresses during the multistage compression test were measured using the Gleeble 3800 thermo-mechanical simulator. To describe the hot-working behaviour, the steel was compressed to the various amount of deformation (4x0.29, 4x0.23 and 4x0.19). The microstructure evolution in successive stages of deformation was determined in metallographic investigations using light, scanning and electron microscopy as well as X-ray diffraction.
Findings: The steel has austenite microstructure with annealing twins and some fraction of ε martensite plates in the initial state. The flow stresses are much higher in comparison with austenitic Cr-Ni and Cr-Mn steels and slightly higher compared to Fe-(15-25) Mn alloys. The flow stresses are in the range of 200-400 MPa for the applied conditions of hot-working. Making use of dynamic and metadynamic recrystallization, it is possible to refine the microstructure and to decrease the flow stress to 350 MPa during the last deformation at 850°C. Applying the true strains of 0.23 and 0.19 requires the microstructure refinement by static recrystallization. After the grain refinement due to recrystallization, the steel is characterised by uniform structure of γ phase without ε martensite plates.
Research limitations/implications: To fully describe the hot-working behaviour of the new-developed steel, further investigations in wider temperature and strain rate ranges are required.
Originality/value: The hot-deformation resistance and microstructure evolution in various conditions of hot-working for the new-developed high-manganese 27Mn-4Si-2Al-Nb-Ti austenitic steel were investigated.
Keywords: High-manganese steel; Hot-working; Compression test; Dynamic recrystallization; Static recrystallization

Reference to this paper should be given in the following way:
L.A. Dobrzański, W. Borek, Processes forming the microstructure evolution of high-manganese austenitic steel in hot-working conditions, Journal of Achievements in Materials and Manufacturing Engineering 37/2 (2009) 397-407.

1. Introduction

Automotive industry belongs to one of the main branches of the global market which creates continuous demands of constructional materials with higher strength conserving required technological formability. Presently, the most advanced steels predicted to be used for the most challenging car components with a complex shape and absorbing energy in crash events are high-manganese austenitic TRIP/TWIP steels [1-6].

Beneficial combination of high strength and ductile properties of these steels depends on structural processes taking place during cold plastic deformation, which are a derivative of stacking fault energy (SFE) of austenite, dependent, in turn on the chemical composition of steel and deformation temperature [1-4, 7-10]. In case, when SFE is equal from 12 to 20mJm^{-2}, partial transformation of austenite into martensite occurs, making use of TRIP effect (TRansformation Induced Plasticity) [1-4, 8]. Values of SFE from 20 to 60mJm^{-2} determine intense mechanical twinning connected to TWIP effect (TWinning Induced Plasticity) [5-10]. The steels cover a very wide carbon concentration in a range from about 0.03 to 1 wt.%, 15-30% Mn, 0-4% Si, 0-8% Al.

The best conditions for obtaining the total elongation up to 80%, due to a gradual increase of mechanical twins, acting as obstacles for dislocation glide, occur when the carbon concentration is in the range of 0.4-0.8% and manganese from 17 to 22% [5, 11, 12]. However, high carbon content may lead to formation of M_3C and $M_{23}C_6$-type carbides, which precipitating on austenite grain boundaries negatively affect the strength and toughness of the steel [11]. Moreover, in the Fe-(17-22) Mn-(0.4-1) C steel grades, besides the formation of deformation twins during straining, a technologically undesirable jerky flow, which presents the features of dynamic strain aging and PLC (Portevin-LeChatelier) effect is observed [6]. Because of these reasons, Frommeyer et al. [1-4] proposed a group of high-manganese steels with carbon content, less than 0.1%. Lower hardening due to decreased carbon concentration was compensated by Si and Al additions, which together with Mn decide about SFE of the alloy and the main deformation mechanism. In a case of Mn $\geq$ 25%, the mechanical properties are mainly dependent on TWIP effect [1, 3, 13] and for Mn $\leq$ 20%, a process influencing a mechanical properties level is strain-induced martensitic transformation of austenite [2-4]. For the latter the initial structure is consisted of γ phase as a matrix, some fraction of ε martensite and sometimes ferrite [2-4].

Results of our earlier investigations [14-17] indicate that ε martensite plates can appear in the initial structure of the (0.04-0.05) C-25Mn-4Si-2Al alloys as a result of Nb and Ti microadditions. The amount of C combined in precipitated carbonitrides reduces its content in the solid solution, thus decreasing the SFE of austenite and resulting in a presence of ε martensite despite high manganese concentration in the investigated steels. It was found [16-18] that the fraction of ε martensite plates is also dependent on a grain size of the γ phase and hot-working conditions. It was also observed that the fraction of mechanical twins within the austenite grains corresponds to the initial grain size, and at the same time affects the mechanical properties [5].

The hot-working behaviour of high-manganese steels is of primary importance for elaborating manufacturing methods consisted of hot rolling and successive cooling to room temperature. However, their hot work hardening and microstructural evolution controlled by thermally activated processes removing it, did not draw much attention compared to cold-working behaviour. Niewielski [19] compared the flow resistance of the 0.5C-17Mn-16Cr austenitic steel with conventional stainless steel of 18-8 type. He observed that the hardening intensity of Cr-Mn steel is much higher than in case of Cr-Ni steel. The difference in a course of work-hardening comes from a different ability of dislocations to splitting and association during straining.

High strain hardening rate is a result of the ability of manganese austenite for dislocation dissociation in the initial deformation stage [19, 20]. The reason for high hardening intensity of Cr-Mn steel are much higher flow stress values compared to Cr-Ni steel, however at lower deformation value of ε_{max} corresponding to maximal flow stress. For example, the yield stress of the Cr-Mn steel hot-twisted at a temperature of 1100°C with a strain rate of 1s^{-1} is equal to 134MPa for the value ε_{max} = 0.18 and increases to 280MPa for ε_{max} = 0.23 with decreasing the deformation temperature to 900°C [19]. Cabanas et al. [21] investigated the retarding effect of Mn content up to 20 wt.% on the grain boundary migration and dynamic recrystallization in binary Fe-Mn alloys. The influence of Al addition on the flow behaviour of 0.1C-25Mn-(0-8) Al alloys was the aim of investigations undertaken by Hamada et al. [22, 23]. They found that flow resistance is slightly higher for the 25Mn3Al than for the 25Mn steel. Moreover, they observed that the flow stress of the austenitic alloys containing Al up to 6% is much higher compared to the steel containing 8% Al with a duplex austenitic-ferritic structure [22]. Investigation results by Hamada et al. [22, 23], Sabet et al. [24] on 0.13C-29Mn-2.4Al steel and Kliber et al. [25] on (0.6-1)C-(17-20)Mn steels confirmed the high work hardening rate of high-manganese alloys in the deformation range lower than ε_{max}, likewise for Cr-Mn steels investigated by Niewielski [19].

For manufacturing methods elaborating, it is especially important that relatively low values of ε_{max} give the opportunities to refine austenitic structures in successive stages of hot-working. Unfortunately, the flow resistance of high-Mn steels is usually investigated under conditions of continuous compression or torsion [20-25]. To determine the softening kinetics, the double- or triple-deformation tests are rarely carried out [22, 25]. Hot-rolling of sheets consists of many passes characterized by the changing amount of deformation and strain rate from pass to pass. This means that the flow stresses should be determined during multi-stage straining testing and for various deformation values. In earlier investigations [14-16, 26, 27] we characterized the force-energetic parameters of hot-working of new-developed low-carbon high-Mn-Si-Al steels in continuous and four-stage compression tests. The aim of the paper is to describe in details the microstructure evolution and phase composition of 0.04C-27Mn-4Si-2Al-Nb-Ti steel subjected to four-stage compression with various amount of deformation.

2. Experimental procedure

Investigations were carried out on new-developed low-carbon high-manganese austenitic 27Mn-4Si-2Al steel containing Nb and Ti microadditions (Table 1). Melts were prepared in the Balzers VSG-50 vacuum induction furnace. After homogenization at 1200°C for 4 h to remove the segregation of Mn, ingots with a mass of 25kg were submitted for open die forging on flats with a width of 220 mm and a thickness of 20 mm. Then, cylindrical machined samples ∅10x12mm were compressed in the

Table 1.
Chemical composition of the investigated steel

27Mn-4Si-2Al-Nb-Ti				Mass contents, (%)			
C	Mn	Si	Al	P	S	Nb	Ti
0.04	27.5	4.18	1.96	0.002	0.017	0.033	0.009

temperature range from 1100 to 850°C using the DSI Gleeble 3800 thermomechanical simulator, used as laboratory equipment of the Institute for Ferrous Metallurgy in Gliwice [28].

In order to determine σ-ε curves, the four-stage compression tests were carried out. The temperatures of the successive deformations were 1100, 1050, 950 and 850°C. The details of the hot-working are given in Table 2. To simulate various conditions of hot-rolling, the amount of true stain were 0.29, 0.23 and 0.19. The time of the isothermal holding of the specimens at a temperature of the last deformation was between 0 and 64s. The specimens were inserted in a vacuum chamber, where they underwent resistance-heating. Tantalum foils were used to prevent from sticking and graphite foils used as a lubricant. The processes controlling the course of work-hardening were evaluated on a basis of the shape of σ-ε curves and structure observations of the specimens water-quenched on different stages of compression. To determine metallographically recrystallization progress at the interval between passes, a part of the specimen was water-cooled after isothermal holding of the specimens compressed at 900°C and 1000 °C with the amount of true strain of 0.29 and 0.5 and a strain rate of $10s^{-1}$.

Metallographic investigations were performed on LEICA MEF4A optical microscope. In order to reveal the austenitic structure, samples were etched in nitric and hydrochloric acids mixture in 2:1 proportion as well using a mixture of nitric acid, hydrochloric acid and water in 2:2:1 proportion. The structure of the investigated steel was also characterised using the SUPRA 25 scanning electron microscope and the JEOL JEM 3010 transmission electron microscope working at accelerating voltage of 300 kV. TEM observations were carried out on thin foils. The specimens were ground down to foils with a maximum thickness of 80 μm before 3 mm diameter discs were punched from the specimens. The disks were further thinned by ion milling method with the Precision Ion Polishing System (PIPS™), using the ion milling device (model 691) supplied by Gatan until one or more holes appeared. The ion milling was done with argon ions, accelerated by voltage of 15 kV.

X-ray diffraction analysis of specimens in the initial state and after various stages of deformation was carried out using the Co Kα radiation in the X'Pert PRO diffractometer with the X'Celerator strip detector.

3. Results and discussion

The structure of the investigated steel in the initial state after forging is shown in Fig. 1. Increased concentration of silicon up to 4% and its influence on the decreasing the stacking fault energy of austenite result in the presence of some fraction of ε martensite in the austenite matrix containing many annealing twins. The ε martensite is present in a form of parallel plates inside austenite grains with a mean grain diameter of about 120 μm (Fig. 1b). The martensite plates are hampered by austenite grain or annealing twins boundaries. The presence of ε martensite is confirmed by X-ray diffraction pattern in Fig. 1a.

It was shown in the earlier experiments [16, 26] that the investigated steel under conditions of continuous hot-compression is characterised by relatively high values of flow stress. For the deformation temperature in a range from 850 to 1050°C, flow stresses of the specimens compressed with a strain rate of 10 s^{-1} are equal from 240 to 450MPa (Table 3). These values are considerably higher than for conventional Cr-Ni and Cr-Mn austenitic steels [19, 20] as well as compared to binary Fe-Mn alloys [21, 22, 24]. A decrease of the deformation temperature by 100°C results in an increase in both the peak stress σ_{max} by about 100 MPa and the peak strain ε_{max}. It is difficult to compare directly ε_{max} values with other austenitic steels, mainly due to the differences in strain rate applied, but it is rather clear that they are smaller in comparison with Cr-Ni, Cr-Mn and Fe-Mn steels [19, 21]. The relatively low values of ε_{max} create convenient conditions to refine the austenite microstructure during hot-rolling by dynamic recrystallization process, especially at a temperature higher than 950°C corresponding to the value of ε_{max} = 0.32 (Table 3). Dynamic recrystallization behaviour, which is typical for alloys with low SFE energy is additionally enhanced comparing to pure Fe-Mn and Fe-Mn-Al alloys by 4% Si, decreasing the stacking fault energy of austenite.

Table 2.
Parameters of the thermo-mechanical treatment carried out in the Gleeble simulator

No	T_A, °C	Deformation I			Cooling I - II		Deformation II			Cooling II - III		Deformation III			Cooling III - IV		Deformation IV			$t_{isother}$ at 850°C, s	Final cooling
		T_1 °C	φ_1	$\dot{\varphi}_1$ s^{-1}	V_1 °C/s	t_1 s	T_2 °C	φ_2	$\dot{\varphi}_2$ s^{-1}	V_2 °C/s	t_2 s	T_3 °C	φ_3	$\dot{\varphi}_3$ s^{-1}	V_3 °C/s	t_3 s	T_4 °C	φ_4	$\dot{\varphi}_4$ s^{-1}		
1	1100	1100	0.29	7	5	10	1050	0.29	8	10	10	950	0.29	9	14	7	850	**0.29**	10	**0**	Water
2	1100	1100	0.29	7	5	10	1050	0.29	8	10	10	950	0.29	9	14	7	850	**0.29**	10	**4**	
3	1100	1100	0.29	7	5	10	1050	0.29	8	10	10	950	0.29	9	14	7	850	**0.29**	10	**16**	
4	1100	1100	0.29	7	5	10	1050	0.29	8	10	10	950	0.29	9	14	7	850	**0.29**	10	**32**	
5	1100	1100	0.29	7	5	10	1050	0.29	8	10	10	950	0.29	9	14	7	850	**0.29**	10	**64**	
6	1100	1100	0.29	7	5	10	1050	0.29	8	10	10	950	0.29	9	14	7	-	-	-	-	
7	1100	1100	0.23	7	5	10	1050	0.23	8	10	10	950	0.23	9	14	7	850	**0.23**	10	32	
8	1100	1100	0.19	7	5	10	1050	0.19	8	10	10	950	0.19	9	14	7	850	**0.19**	10	32	

T_A – austenitizing temperature, $T_{1...}$- T_4 – deformation temperatures, $\varphi_{1...}$- φ_4 – true strains, V_1…- V_4 – cooling rates between deformations, $t_{1...}$- t_3 – times between deformations, $t_{isother}$ – time of the isothermal holding of the specimens at a temperature of 850°C

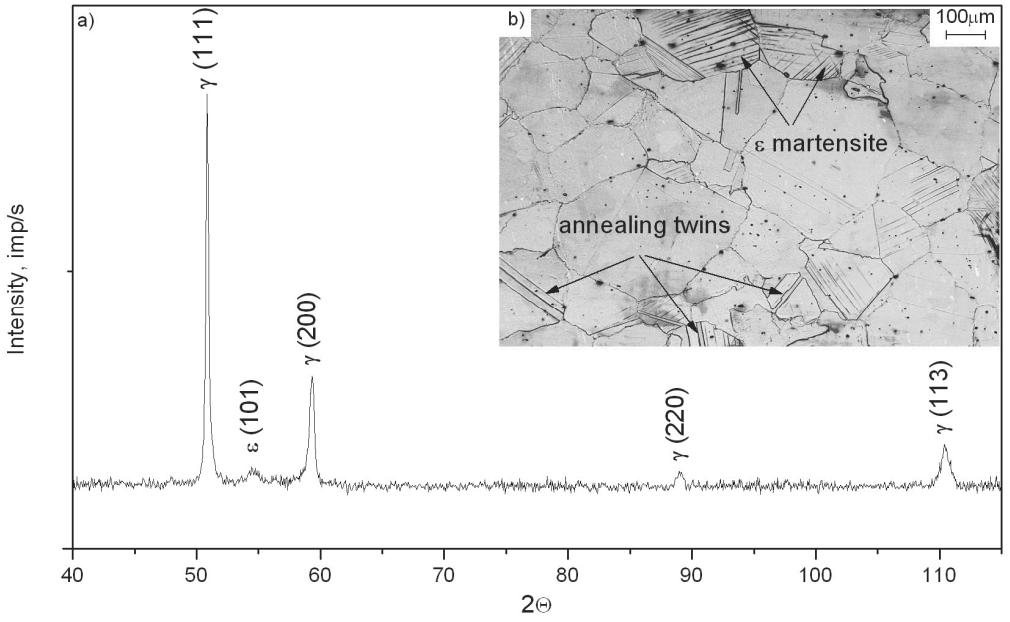

Fig. 1. X-ray diffraction pattern (a) and the austenite structure with many annealing twins and parallel ε martensite plates of the investigated steel in the initial state (after forging) (b)

Table 3.
Influence of the deformation temperature on the ε_{max} strain and maximum flow stress values for the specimens compressed with a strain rate of $10s^{-1}$ [16]

T, °C	ε_{max}	σ_{max}, MPa
1050	0.23	240
950	0.32	350
850	0.48	450

Stress-strain curves of the steel plastically deformed according to the schedule shown in Table 2 are presented in Fig. 2. Application of true strain equal 0.29 during multi-stage compression creates possibility in the course of dynamic recrystallization, what is indicated by peaks that can be distinguished on σ-ε curves – especially for deformations realized at temperature of 1100 and 1050°C. After decreasing deformation temperature to 950 and 850°C, maxima on σ-ε curves are present for a value of true strain nearly 0.29. The values of flow stress of the specimen deformed at 1050°C and corresponding true strain are comparable with values obtained in continuous compression test (Table 3). However, after decreasing the compression temperature to 950°C, both the flow stress and ε_{max} strain are smaller, compared to values in Table 3. It is especially evident after further temperature decrease to 850°C (Fig. 2). The maximum flow stress value is 380 MPa and corresponding peak strain is about 0.28. These values are much smaller compared to 450 MPa and ε_{max} = 0.48 obtained during continuous compression (Table 3). Faster recrystallization initiation and lower flow stress values are probably a result of austenite grain refinement [19] due to cyclic deformation and partial recrystallization between successive deformations. The austenite microstructure directly before the fourth deformation is shown in Fig. 3b. The similar effect due to cyclic compression was observed in [25].

The microstructure evolution in different stages of multi-stage compression is shown in Fig. 3. After deformation of the specimen at a temperature of 950°C and subsequent cooling for 7s corresponding to the interpass time, the steel is characterised by uniform, metadynamically recrystallized austenite microstructure with a mean grain size of about 20μm and many annealing twins (Fig. 3a, b). The initiation of dynamic recrystallization during the last deformation at the temperature of 850°C is confirmed by a micrograph in Fig. 3c, showing an initial state of dynamic recrystallization. The mean dynamically recovered austenite grain size decreased to about 12μm and fine dynamically recrystallized grains are arranged along austenite grain boundaries as well as on twin boundaries (Fig. 3d). The similar role of twinning as a nucleation and growth mechanism of dynamic recrystallization was observed by Sabet et al. [24] in Fe-29Mn-2.4Al alloy. The repeated formation of twins during the whole temperature range of hot-working may be a reason of amplification of a number of dynamically recrystallized grains. The annealing twins are present both inside large dynamically recovered grains and fine recrystallized grains (Fig. 3d). A low tendency of high-manganese austenite with a low SFE to dynamic recovery is confirmed by Fig. 4, revealing a weakly outlined cellular dislocation structure in a region still not subjected to dynamic recrystallization, despite the true strain of 0.29, slightly higher than corresponding to a maximal value of true stress. The analysis of Fig. 4 allows to reveal the highly deformed austenite structure with a various density of crystal structure defects, where inside, it is possible to observe regions with a much lower dislocation density corresponding to a state directly before forming dynamic recrystallization nuclei. A lack of distinct cellular dislocation structure in metals with low SFE is due to the necessity of extended dislocations to recombine it to a perfect dislocation before the cross slip initiation, what requires providing activation energy, dependent on normalized stacking fault energy of γ phase.

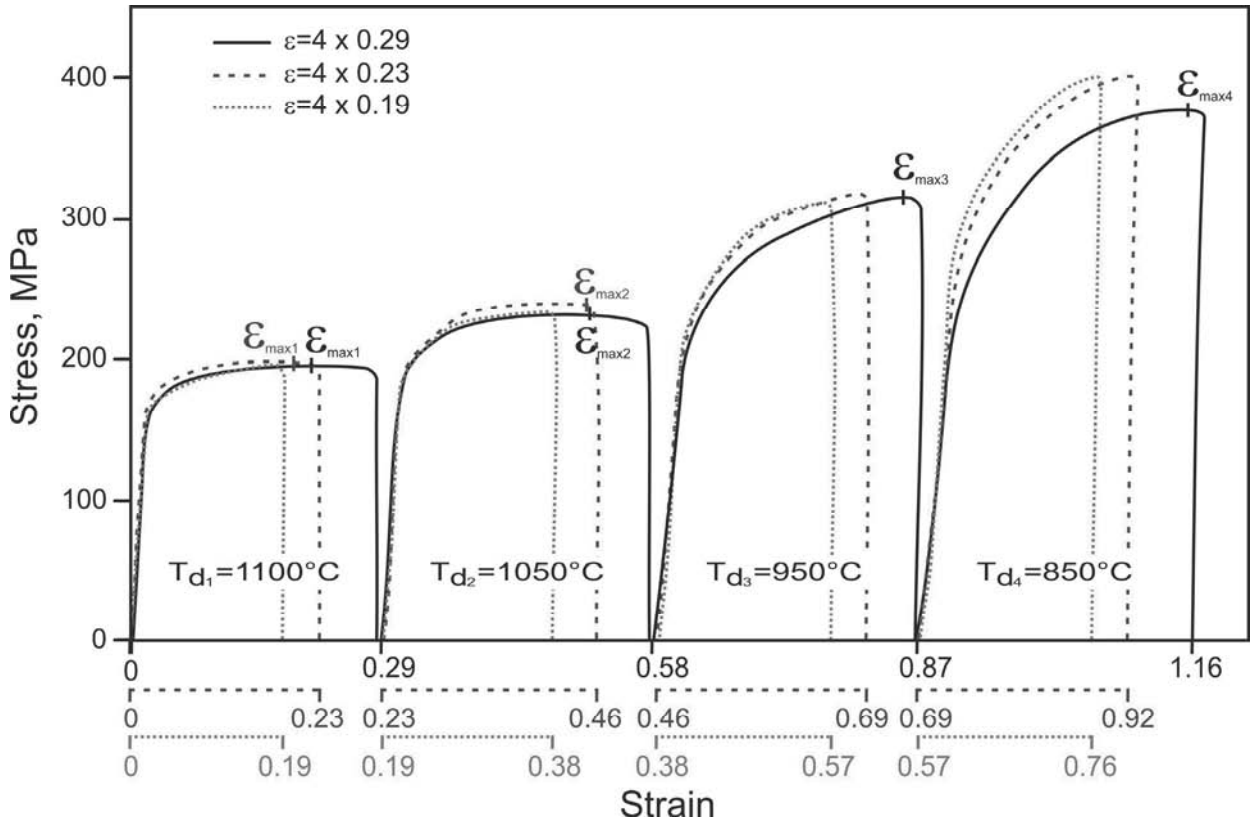

Fig. 2. Stress - strain curves after the multi-stage compression of the axisymetrical specimens deformed with the true strain 4x0.29, 4x0.23 and 4x0.19 in a temperature range from 1100 to 850°C; the strain axis was interrupted for the true strains of 4x0.23 and 4x0.19 in order to compare the σ-ε curves with that deformed 4x0.29

Isothermal holding of the specimen at a temperature of the last deformation for 16s leads to growth of new grains as a result of metadynamic recrystallization and the initiation of static recrystallization on grain boundaries of large, flattened austenite grains whose fraction is still high (Fig. 3e,f). Further increase in the isothermal holding time to 32s leads to obtain nearly 60% fraction of metadynamically and statically recrystallized microstructure with a mean austenite grain size of about 10μm (Fig. 3g,h).

The fraction of the recrystallized phase in intervals between successive passes can be evaluated from Fig. 5a, showing a progress of recrystallization as a function of time for the specimens compressed in various deformation conditions. For example, the time for half-recrystallization of the steel deformed to the true strain of 0.5 at a temperature of 1000°C is about 12s. Decrease in the deformation temperature to 900°C results in increase of the $t_{0.5}$ time to about 16s (Fig. 5a), what corresponds mainly to a course of metadynamic recrystallization of austenite. Decreasing the true strain to 0.29 corresponding to applied one during four-stage compression, causes further increase in the half-recrystallization time to about 31s. Slower progress of recrystallization is a result of a lower true strain value. Under these deformation conditions, the reconstruction of microstructure proceeds mainly by static recrystallization, which requires certain incubation period.

However, the curve in Fig. 5a and the microstructure of the steel isothermally held for 4s at 900°C (Fig. 5b) indicate some fractions of recrystallized grains. Due to short time applied, it is a result of metadynamic recrystallization, not required incubation time to proceed. The relatively small fraction of new, fine grains after increasing the holding time to 16s is due to relatively slow progress of static recrystallization (Fig. 5c). It is also confirmed by a small fraction of statically recrystallized grains obtained after isothermal holding for 16s of the specimen subjected to four-stage compression (Fig. 3e, f). Hamada et al. [22] observed that the high addition of Mn retards the static recrystallization rate significantly and the activation energy of static recrystallization is higher than typical values reported for low-alloyed C-Mn steels but lower compared to Cr-Ni stainless steels. Increase of holding time to 64s leads to achievement of highly fine-grained microstructure of metadynamically and statically recrystallized grains (Fig. 5d).

It is interesting that in Fig. 3 any ε martensite plates were observed, despite presence of this phase in the initial structure (Fig. 1). Confirmation of that fact is the X-ray diffraction patterns shown in Fig. 6 for different stages of thermo-mechanical treatment. A lack of ε martensite is connected with significant structure refinement compared to the initial state and hampering influence of grain boundaries on growth of ε martensite plates during cooling. Similar effects were reported in [18] for Fe-21Mn alloy and in [22] for Fe-25Mn alloy.

a) 950°C-7s-850°C-water

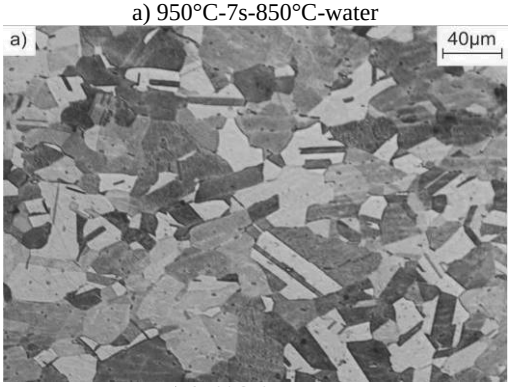

b) 950°C-7s-850°C-water

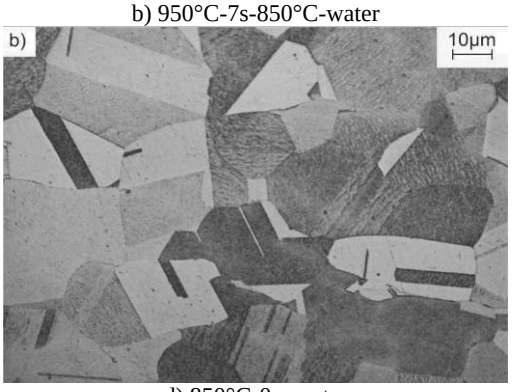

c) 850°C-0s- water

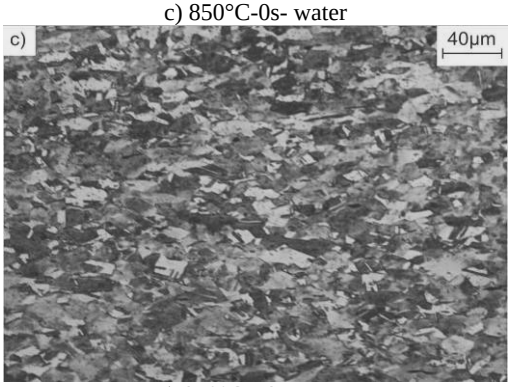

d) 850°C-0s- water

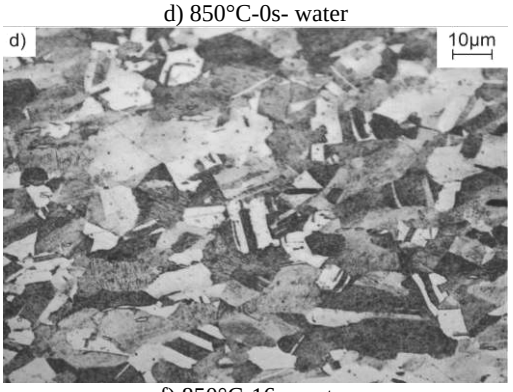

e) 850°C-16s- water

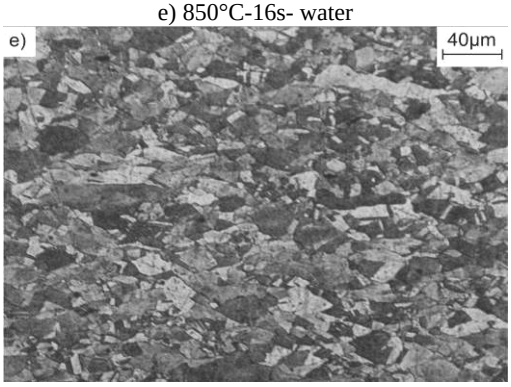

f) 850°C-16s- water

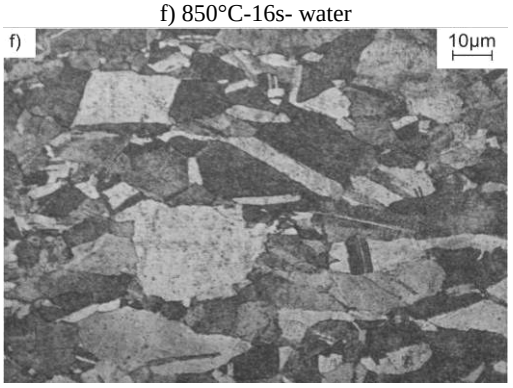

g) 850°C-32s- water

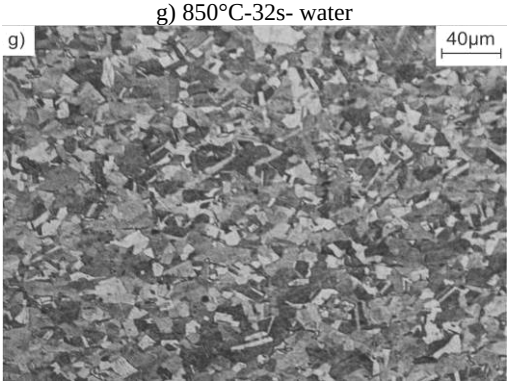

h) 850°C-32s- water

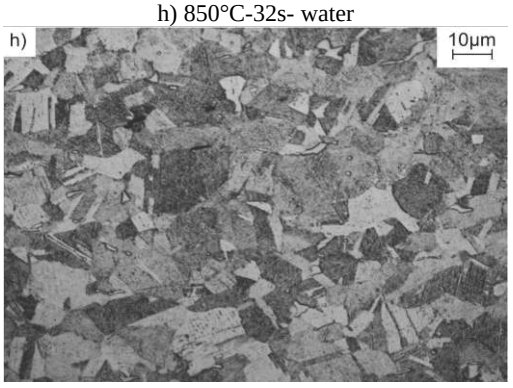

Fig. 3. Austenitic structures obtained after steel solutioning at successive stages of the hot-working for the specimens compressed to a true strain of 4x0.29 and isothermally held for the time from 0 to 32s: a, b) metadynamically recrystallized grains during the interval between third and fourth deformation, c, d) initiation of dynamic recrystallization, e, f) grain refinement mainly due to metadynamic recrystallization, g, h) grain refinement due to metadynamic and static recrystallization

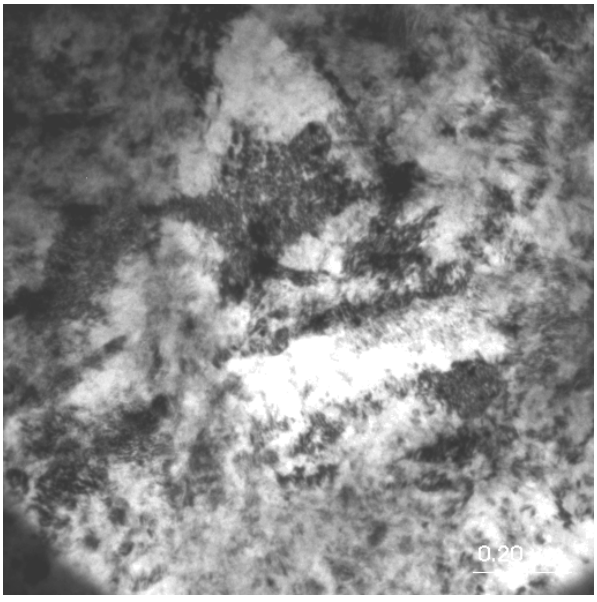

Fig. 4. Regions of dynamically recovered austenite with a various dislocation density of the steel solution heat-treated from a temperature of 850°C directly after the true strain of 4x0.29

Due to high rolling forces in final passes of sheet rolling, the amount of deformation is usually reduced. Because of this the four-stage compression with true strains of 4x0.23 and 4x0.19 were also carried out. Decrease of true strain to 0.23 leads to a change of the course of σ-ε curves (Fig. 2). In order to compare the curves course, the strain axis was interrupted. A shape of the curves during deformation in a temperature range of 1100-1050°C and true stress values are comparable to that obtained after higher strain applying. Moreover, the applied strain is sufficient to initiate a course of dynamic recrystallization. However, decreasing the compression temperature to 950°C causes that the flow stress is slightly higher and the applied strain value is too low to initiate dynamic recrystallization. Thus, process controlling a course of hot-working at 950°C is a dynamical recovery.

Further decrease in the deformation temperature results in a further increase of the true stress to a value of about 50 MPa higher compared to the specimen deformed under conditions of dynamic recrystallization. This is due to only partial course of static recrystallization when cooling a sample between third and fourth deformation. Because of a lack of dynamic recrystallization in final passes, a refinement of microstructure requires the use of thermally activated, static processes removing work-hardening. For instance, the micrographs in Fig. 7 show the austenite microstructure of the steel isothermally held for 32 s at 850°C after compression with a true strain of 4x0.23. The fraction of statically recrystallized austenite equals approximately 60% (Fig. 7a). Numerous annealing twins can be observed in the microstructure (Fig. 7b) and a mean statically recrystallized austenite grain is higher compared to the specimen compressed 4x0.29, where a reconstruction of the microstructure was obtained both in static and metadynamic processes (Fig. 3h).

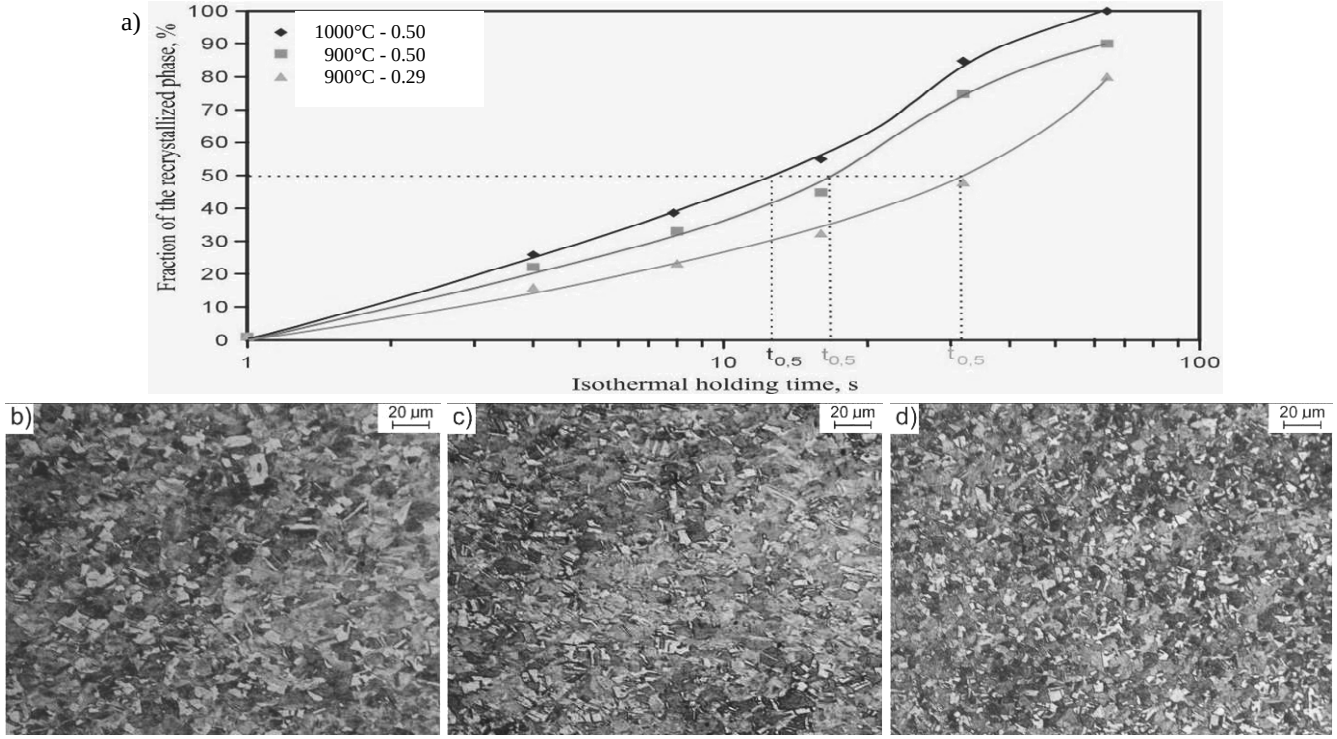

Fig. 5. Progress of recrystallization of the investigated steel isothermally held after plastic deformation in various conditions (a); and microstructure evolution of the steel isothermally held for the time: b) t = 4s; c) t = 16s; d) t = 64s after the true strain of 0.29 at 900°C

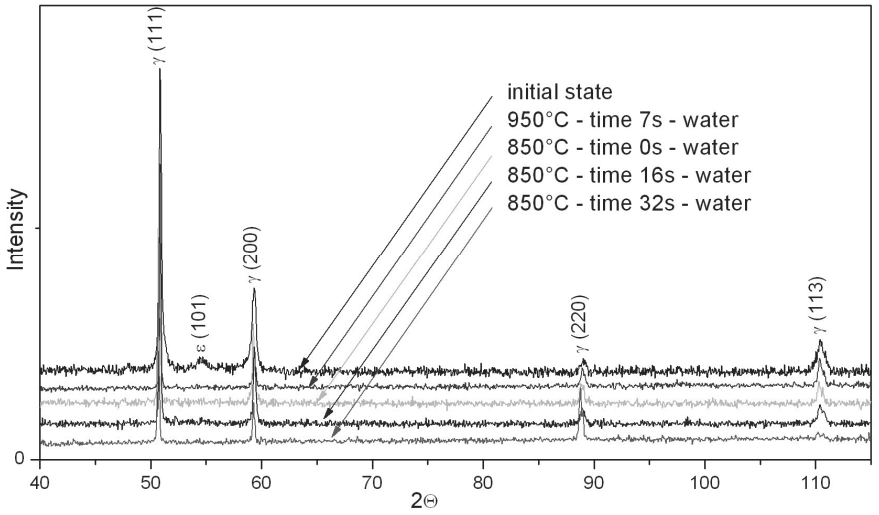

Fig. 6. X-ray diffraction patterns of the steel in the initial state and after different stages of thermo-mechanical treatment

a) 850°C-32s- water

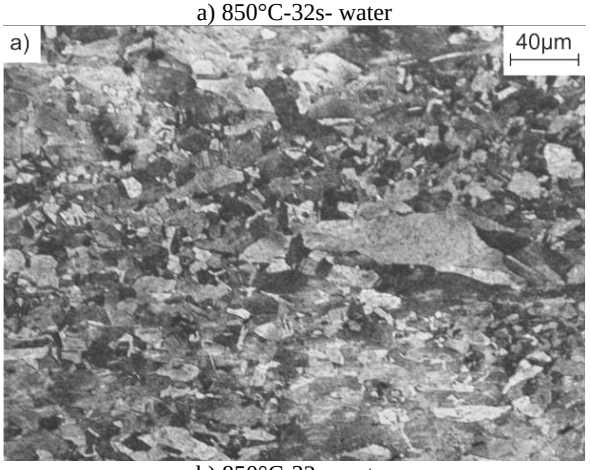

b) 850°C-32s- water

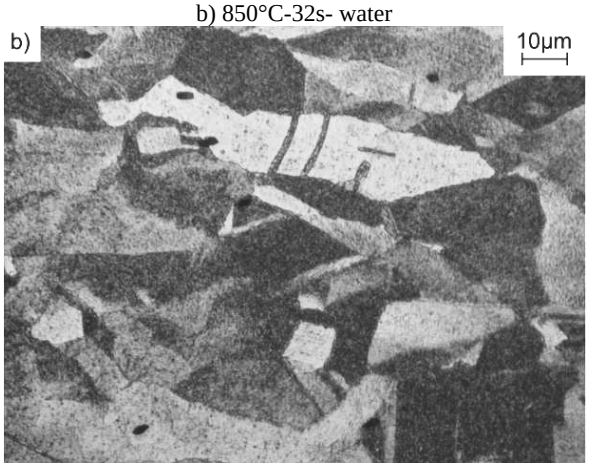

Fig. 7. Fine, statically recrystallized austenite grains and large statically recovered grains of the steel solution heat-treated from a temperature of 850°C after isothermal holding for 32 s of the specimen compressed with the true strain of 4x0.23 (a, b)

Relatively slow progress of static recrystallization is a result of impeding influence of high content of solutes on the migration of grain boundaries. The statically recovered, deformed austenite grains have low tendency to form a cellular dislocation structure, likewise dynamically recovered grains (Fig. 4). Inside these grains, regions characterized by various dislocation density can be observed (Fig. 8).

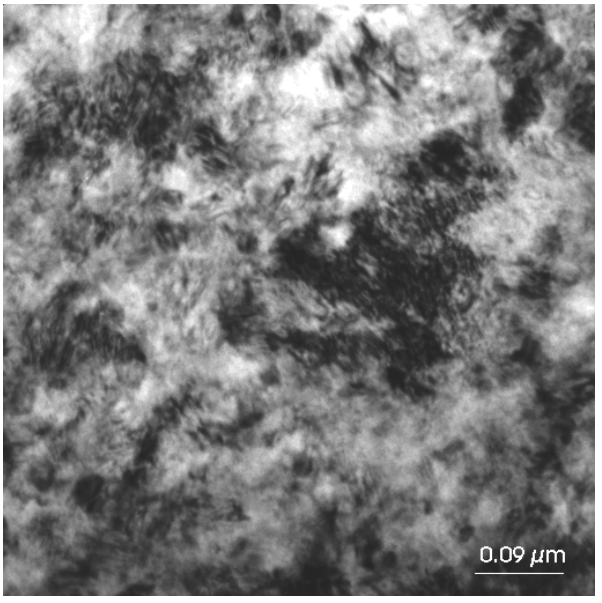

Fig. 8. Regions of statically recovered austenite with a various dislocation density of the steel solution heat-treated from the temperature of 850°C after isothermal holding for 32 s of the specimen compressed with the true strain of 4x0.23

A decrease of true strain to 0.19 causes that dynamic recovery is the process controlling strain hardening in the whole

temperature range of deformation (Fig. 2), at similar values of flow stress in comparison with the specimen deformed 4x0.23. However, the isothermal holding of the specimen for 32 s is too short to obtain a desired fraction of recrystallized phase, which equals approximately 15% (Fig. 9a). Fine, recrystallized grains are located mainly on grain boundaries of large, flattened statically recovered grains (Fig. 9b). Both recrystallized and recovered grains are bigger than those after applying the true strain being equal 0.23 (Fig. 7). Once again, numerous annealing twins can be observed in the microstructure (Fig. 9a, b). The microstructure in Fig. 10 clearly shows that new grains are located on grain boundaries of large, statically recovered austenite grains. Moreover, a jerky-like character of the boundaries of large grains can be observed. It is a characteristic feature of a state directly before forming a recrystallization nucleus [19].

a) 850°C-32s-water

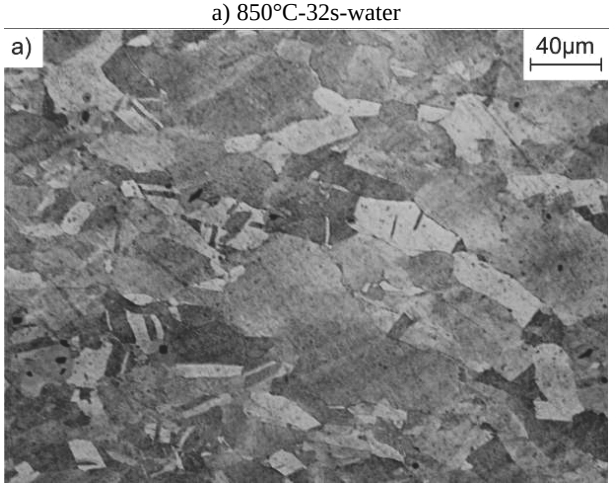

b) 850°C-32s-water

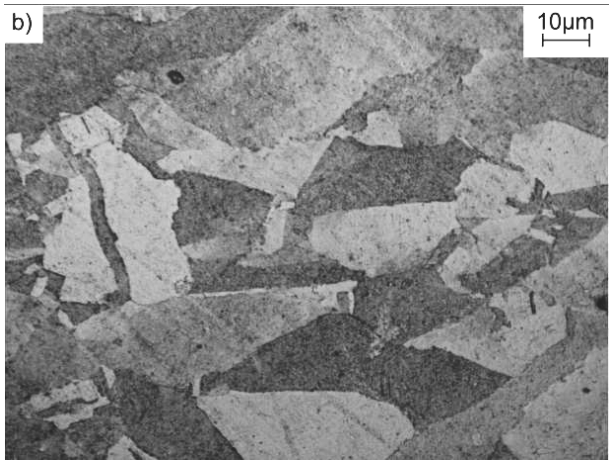

Fig. 9. Fine, statically recrystallized austenite grains and large statically recovered grains of the steel solution heat-treated from the temperature of 850°C after isothermal holding for 32 s of the specimen compressed with the true strain of 4x0.19 (a, b)

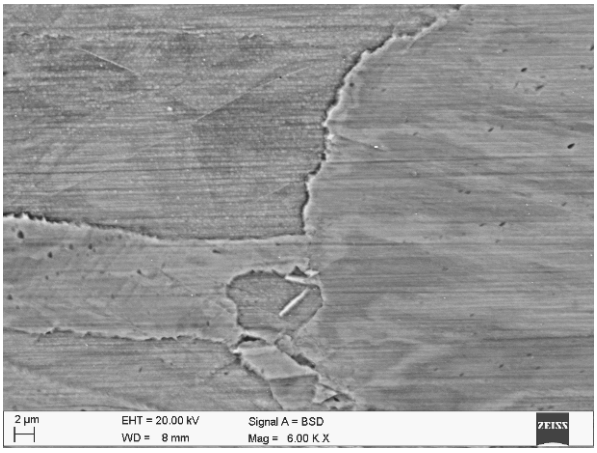

Fig. 10. The fine, statically recrystallized grain on jerky-like boundaries of three large, statically recovered grains of the steel solution heat-treated from the temperature of 850°C after isothermal holding for 32 s of the specimen compressed with the true strain of 4x0.19

4. Conclusions

On the basis of the investigations carried out in the initial state and under conditions of the continuous and multi-stage compression, the following conclusions can be drawn:

- The new-developed 27Mn-4Si-2Al-Nb-Ti steel in the initial state has the austenitic structure with many annealing twins and some fraction of ε marteniste plates, impeded by grain and twins boundaries. Essential influence on the presence of ε martensite have Nb and Ti microadditions causing the decrease of stacking fault energy of γ phase by fixing carbon. The decrease of SFE is also enhanced by addition of 4% Si.
- The hot-working resistance of the steel is much higher in comparison with austenitic Cr-Ni and Cr-Mn steels and slightly higher compared to binary Fe-Mn alloys. The flow stresses are in the range of 200-400 MPa for the applied conditions of hot-working and are up to 80 MPa lower compared to continuous compressions.
- The best conditions for a gradual grain refinement occur after four-stage compression with the true strain of 4x0.29 in hot-working conditions controlled by dynamic recrystallization in a whole temperature deformation range. The steel solutioned directly after deformation is characterized by a mixture of fine, recrystallized grains and some fraction of dynamically recovered grains with a mean diameter of about 12 μm. Completing recrystallization in all the deformed grains requires isothermal holding of the specimen for 32 s at 850°C. The refinement of austenite microstructure proceeds by metadynamic recrystallization.
- Decreasing the true strain to 4x0.23 and 4x0.19 changes a main mechanism controlling a course of work hardening from dynamic recrystallization to dynamic recovery. A relatively small fraction of recrystallized phase between successive passes is a reason of higher flow stresses up to

400 MPa in a final deformation temperature. Due to slow progress of static recrystallization, the isothermal holding of the specimens at 850°C for 32 s results in a small fraction of recrystallized austenite and a larger size of flattened, statically recovered grains.

- High-manganese austenite with a low SFE has a low tendency to dynamic recovery and forming a distinct cellular dislocation structure.
- Repeated recrystallization and corresponding grain refinement causes that the thermo-mechanically processed steel is characterized by uniform structure of γ phase without ε martensite plates.

Acknowledgements

Scientific work was partially financed from the science funds in a period of 2009-2011 in the framework of project No. N N507 287936.

The authors would like to express their gratitude to Prof. R. Kuziak of Institute for Ferrous Metallurgy in Gliwice for carrying out the experiments using the Gleeble 3800 simulator.

References

[1] G. Frommeyer, U. Brüx, K. Brokmeier, R. Rablbauer, Development, microstructure and properties of advanced high-strength and supraductile light-weight steels based on Fe-Mn-Al-Si-(C), Proceedings of the 6th International Conference on Processing and Manufacturing of Advanced Materials, Thermec'2009, Berlin, 2009, 162.

[2] G. Frommeyer, O. Grässel, High strength TRIP/TWIP and superplastic steels: development, properties, application, La Revue de Metallurgie-CIT 10 (1998) 1299-1310.

[3] G. Frommeyer, U. Brüx, P. Neumann, Supra-ductile and high-strength manganese-TRIP/TWIP steels for high energy absorption purposes, ISIJ International 43 (2003) 438-446.

[4] O. Grässel, L. Krüger, G. Frommeyer, L.W. Meyer, High strength Fe-Mn-(Al, Si) TRIP/TWIP steels development – properties – application, International Journal of Plasticity 16 (2000) 1391-1409.

[5] A. Saeed-Akbari, W. Bleck, U. Prahl, The study of grain size effect on the microstructure development and mechanical properties of a high-Mn austenitic steel, Proceedings of the 6th International Conference on Processing and Manufacturing of Advanced Materials, Thermec'2009, Berlin, 2009, 194.

[6] K. Renard, H. Idrissi, S. Ryelandt, F. Delannay, D. Schryvers, P.J. Jacques, Strain-hardening mechanisms in Fe-Mn-C austenitic TWIP steels: Mechanical and micromechanical characterisation, Proceedings of the 6th International Conference on Processing and Manufacturing of Advanced Materials, Thermec'2009, Berlin, 2009, 72.

[7] Y.G. Kim, J.M. Han, J.S. Lee, Composition and temperature dependence of tensile properties of austenitic Fe-Mn-Al-C alloys, Materials Science and Engineering A 114 (1989) 51-59.

[8] S. Allain, J.P. Chateau, O. Bouaziz, S. Migot, N. Guelton, Correlations between the calculated stacking fault energy and the plasticity mechanisms in Fe-Mn-C alloys, Materials Science and Engineering A 387-389 (2004) 158-162.

[9] T. Bator, Z. Muskalski, S. Wiewiórkowska, J.W. Pilarczyk, Influence of the heat treatment on the mechanical properties and structure of TWIP steel in wires, Archives of Materials Science and Engineering 28 (2007) 337-340.

[10] E. Mazancova, I. Schindler, K. Mazanec, Stacking fault energy analysis of the high manganese TWIP and TRIPLEX alloys, Hutnicke Listy 3 (2009) 55-58.

[11] J. Kliber, T. Kursa, I. Schindler, The influence of hot rolling on mechanical properties of high-Mn TWIP steels, 3rd International Conference on Thermomechanical Processing of Steels, TMP'2008, (CD-ROM), Padua, 2008, s.1-12.

[12] J. Kliber, T. Kursa, I. Schindler, Hot rolling of steel with TWIP effect, Metallurgist – Metallurgical News 8 (2008) 481-483.

[13] S. Vercammen, B. Blanpain, B.C. De Cooman, P. Wollants, Mechanical behaviour of an austenitic Fe-30Mn-3Al-3Si and the importance of deformation twinning, Acta Materialia 52 (2004) 2005-2012.

[14] A. Grajcar, W. Borek, The thermo-mechanical processing of high-manganese austenitic TWIP-type steels, Archives of Civil and Mechanical Engineering 8/4 (2008) 29-38.

[15] L.A. Dobrzański, A. Grajcar, W. Borek, Influence of hot-working conditions on a structure of high-manganese austenitic steels, Journal of Achievements in Materials and Manufacturing Engineering 29/2 (2008) 139-142.

[16] L.A. Dobrzański, A. Grajcar, W. Borek, Microstructure evolution and phase composition of high-manganese austenitic steels, Journal of Achievements in Materials and Manufacturing Engineering 31/2 (2008) 218-225.

[17] A. Grajcar, M. Opiela, G. Fojt-Dymara, The influence of hot-working conditions on a structure of high-manganese steel, Archives of Civil and Mechanical Engineering 9/3 (2009) 49-58.

[18] K.K. Jee, J.H. Han, W.Y. Jang, Measurement of volume fraction of ε martensite in Fe-Mn based alloys, Materials Science and Engineering A 378 (2004) 319-322.

[19] G. Niewielski, Changes of structure and properties of austenitic steel caused by hot deformation, Scientific Books of the Silesian University of Technology 58, The Silesian University of Technology Publishers, Gliwice, 2000 (in Polish).

[20] G. Niewielski, M. Hetmańczyk, D. Kuc, Influence of the initial grain size and deformation parameters on the mechanical properties during hot plastic deformation of austenitic steels, Materials Engineering 24/6 (2003) 795-798 (in Polish).

[21] N. Cabanas, N. Akdut, J. Penning, B.C. De Cooman, High-temperature deformation properties of austenitic Fe-Mn alloys, Metallurgical and Materials Transactions A 37 (2006) 3305-3315.

[22] A.S. Hamada, L.P. Karjalainen, M.C. Somani, The influence of aluminium on hot deformation behaviour and tensile properties of high-Mn TWIP steels, Materials Science and Engineering A 467 (2007) 114-124.

[23] A.S. Hamada, L.P. Karjalainen, M.C. Somani, R.M. Ramadan, Deformation mechanisms in high-Al bearing high-Mn TWIP steels in hot compression and in tension at low temperatures, Materials Science Forum 550 (2007) 217-222.
[24] M. Sabet, A. Zarei-Hanzaki, S. Khoddam, An investigation to the hot deformation behaviour of high-Mn TWIP steels, 3rd International Conference on Thermomechanical Processing of Steels, TMP'2008, (CD-ROM), Padua, 2008, s.1-7.
[25] J. Kliber, K. Drozd, Stress-strain behaviour and softening in manganese TWIP steel tested in thermal-mechanical simulator, Hutnicke Listy 3 (2009) 31-36.
[26] L.A. Dobrzański, A. Grajcar, W. Borek, Hot-working behaviour of high-manganese austenitic steels, Journal of Achievements in Materials and Manufacturing Engineering 31/1 (2008) 7-14.
[27] L.A. Dobrzański, A. Grajcar, W. Borek, Microstructure evolution of high-manganese steel during the thermo-mechanical processing, Archives of Materials Science and Engineering 37 (2009) 69-76.
[28] R. Kuziak, Modelling of structure changes and phase transformations occurring in thermo-mechanical processes of steel, Institute for Ferrous Metallurgy, Gliwice, 2005 (in Polish).
[29] L.A. Dobrzański, A. Grajcar, W. Borek, Microstructure evolution of C-Mn-Si-Al-Nb high-manganese steel during the thermomechanical processing, Materials Science Forum (in print).
[30] T. Niendorf, C. Lotze, D. Canadinc, A. Frehn, H.J. Maier, The role of monotonic pre-deformation on the fatigue performance of a high-manganese austenitic TWIP steel, Materials Science and Engineering A 499 (2009) 518-524.